Thermochimica Acta, 24 (1978) 121–131
© Elsevier Scientific Publishing Company, Amsterdam – Printed in The Netherlands

MEASUREMENT OF DILUTE METALLIC IMPURITY CONCENTRATION IN LEAD BY DIFFERENTIAL SCANNING CALORIMETRY*

D. L. DECKER AND R. W. YOUNG
Department of Physics and Astronomy, Brigham Young University, Provo, UT 84602 (U.S.A.)
(Received 20 June 1977)

ABSTRACT

The traditional method for purity determination by analysis of the peak shape of the melting transition has included fitting to a linear relation between sample temperature (T) and the reciprocal fraction molten ($1/\gamma$). This technique, however, necessitates the use of a series of calibrants to determine the proper choice of limits for $1/\gamma$ as a function of purity. In this paper, a non-linear relation between T and $1/\gamma$ is developed and applied to the determination of metallic impurities in Pb in the range of a few to 1000 parts per million. The results are found to be independent of the range of $1/\gamma$ used. The use of differential scanning calorimetry in this determination is discussed, and rate effects are also mentioned.

INTRODUCTION

In the process of measuring the rate of Au diffusion in dilute lead (gold) alloys, it became necessary to find an inexpensive method of determining the amount of Au in the alloy. One cannot assume the concentrations to be the amount placed in the melt because of segregation as the solidification zone moves across the specimen to form a single crystal by the Bridgman technique. Because of the possible non-uniform concentration, it is necessary to measure the concentration at several points along the crystal making the expense of activation analysis prohibitive.

The nature of the melting curve of a pure material is considerably altered as foreign atoms are added to the material. This change can be harnessed to give a quantitative measure of the impurity concentration. One can focus on the shift of the liquidous line with concentration or on the change in the shape of the melting signal itself. For very dilute alloys, the melting temperature shifts are small, and the precision with which one can determine the actual melting temperature is not good enough for accurate determination. Thus we took the later approach. We briefly present the basic theory and its assumptions followed by an analysis of the use of differential scanning

---

* Work supported in part by the National Science Foundation.

calorimetry in making these measurements. Finally, we will present our results and discuss advantages and limitations of this technique.

Differential scanning calorimetry (DSC) has been used in the past to determine impurity concentrations[1-5]. Marti[1] gives a review of the literature on the DSC method for purity determination. All these measurements were based on a linear relation between the temperature and the reciprocal of the fraction of the sample molten, γ.

$$T = T_0 - (x_2 R T_0^2 / \Delta H_f)(1/\gamma) \tag{1}$$

where T_0 is the melting temperature of the pure solvent, R the molar gas constant, x_2 the concentration of the solute, and ΔH_f the heat of fusion of the pure solvent. These earlier experimenters observed a strong effect of scan rate on their calculated impurity concentrations. They also noted that $T(1/\gamma)$ was not linear except for very pure samples. The rate dependence was assumed to be caused by inability of the sample to attain equilibrium at the faster scan rates. Driscol et al.[3] assumed the non-linearity of $T(1/\gamma)$ was due to a portion of the melting peak area being missed before the signal departed measurably from the baseline. They thus proposed a "linearization" procedure but then found their calculated impurity concentrations to depend strongly upon the range of $1/\gamma$ used.

We do not use eqn (1) but derive a relation between T and $1/\gamma$ that is not linear. The impurity concentrations will be shown to have much less rate dependence and will be independent of the range of $1/\gamma$ used in the analysis.

THEORY

In the limit of dilute solutions, the lowering of the melting point is given by[6]

$$\mathrm{d}T/\mathrm{d}x_1 = -RT^2/\Delta H_f \tag{2}$$

where x_1 is the mole fraction of saturated solute in the liquid phase at temperature T and ΔH_f is as defined above. From eqn (2), we see that the lowering of the melting point depends only upon the solute concentration and not upon the nature of the solute, at least for solutes that do not dissociate. This equation assumes that the solute is insoluble in the solid phase. Lewis and Randall[7] have extended eqn (2) to include a system with a finity solubility in the solid phase.

$$\mathrm{d}T/\mathrm{d}x_1 = (k - 1)RT^2/\Delta H_f \tag{3}$$

where k is the distribution coefficient, or the ratio of the solubility in the solid to that in the liquid phase at a given temperature. From the temperature dependence of k, it is seen that, over a small range of temperature near T_c, k is constant[8]. The constancy of k for dilute solutions is known as Nernst's law[7]. Integration of eqn (3) yields

$$T - T_0 = RT_0 T x_1(k - 1)/\Delta H_f \tag{4}$$

Using the law of levers between the liquidous and solidous for an alloy with solute mole fraction x_2, one finds[9]

$$x_1 = x_2/[k + \gamma(1 - k)] \tag{5}$$

where γ is the fraction molten at temperature T. Substitution of (5) into (4) yields, after rearranging,

$$T = T_0 + \kappa T_0/\gamma - (\eta + \kappa)T/\gamma \tag{6}$$

In the above $\eta \equiv RT_0 x_2/\Delta H_f$ and $\kappa \equiv k/(1 - k)$. Letting $x = 1/\gamma$, we have an expression to which we can fit the data by linear least squares techniques.

$$T = A + Bx + CTx \tag{7}$$

with $A = T_0$, $B = \kappa T_0$, and $C = -(\eta + \kappa)$. Note that eqn (7) is not a linear relation between T and $1/\gamma$ as was the former expression, eqn (1), even in the case of no solid solubility.

ANALYSIS AND EXPERIMENTAL PROCEDURE

We shall briefly review how T and γ are obtained from the DSC signal. In each of the matched pans of the DSC are placed identical aluminum containers, one of which contains the lead sample. The output signal from the DSC is the difference in heat flow supplied to the two pans as the pan temperatures are swept together at a constant rate, $\dot{T}_p$. In dynamic thermal measurements such as these, thermal lag between the aluminum containers and the pans is included through Newton's Law which is the thermal equivalent of Ohm's Law[10].

$$T_p - T = R_0(\dot{q} + C_0\dot{T}_p) \tag{8}$$

Here T_p is the pan temperature, T the sample temperature, $\dot{q}$ the DSC signal above the instrumental baseline (see Fig. 1), C_0 the specific heat of the sample and its container, and R_0 the thermal resistance to heat flow from the pan to the container. By conservation of energy during the process of melting the sample, we have

$$\dot{q}_1 = \dot{h} + C_0\dot{T} \text{ and } \dot{q}_2 = (C_0 - C_s)\dot{T}_p \tag{9}$$

where $\dot{q}_1$ is the power dissipated in the pan containing the sample and $\dot{q}_2$ is that in the other pan. $\dot{h}$ is the rate at which heat is used in melting the sample, and C_s is the specific heat of the sample. In the baseline region $\dot{q}_1 - \dot{q}_2 = C_s\dot{T}_p$, because $\dot{T} = \dot{T}_p$ and $\dot{h} = 0$. The signal above the instrumental baseline during melting is

$$\dot{q} \equiv \dot{q}_1 - \dot{q}_2 - C_s\dot{T}_p = \dot{h} + C_0(\dot{T} - \dot{T}_p) \tag{10}$$

The DSC melting signal for a pure sample as a function of time should appear as shown in Fig. 1a. Melting begins at point B. During melting $\dot{T} = 0$, and the signal rises at a constant slope $\ddot{q} = \dot{T}_p/R_0$ which is obtained by differentiating eqn (8) while remembering that $\dot{T}_p$ and T are constant. At point C melting is complete, and the

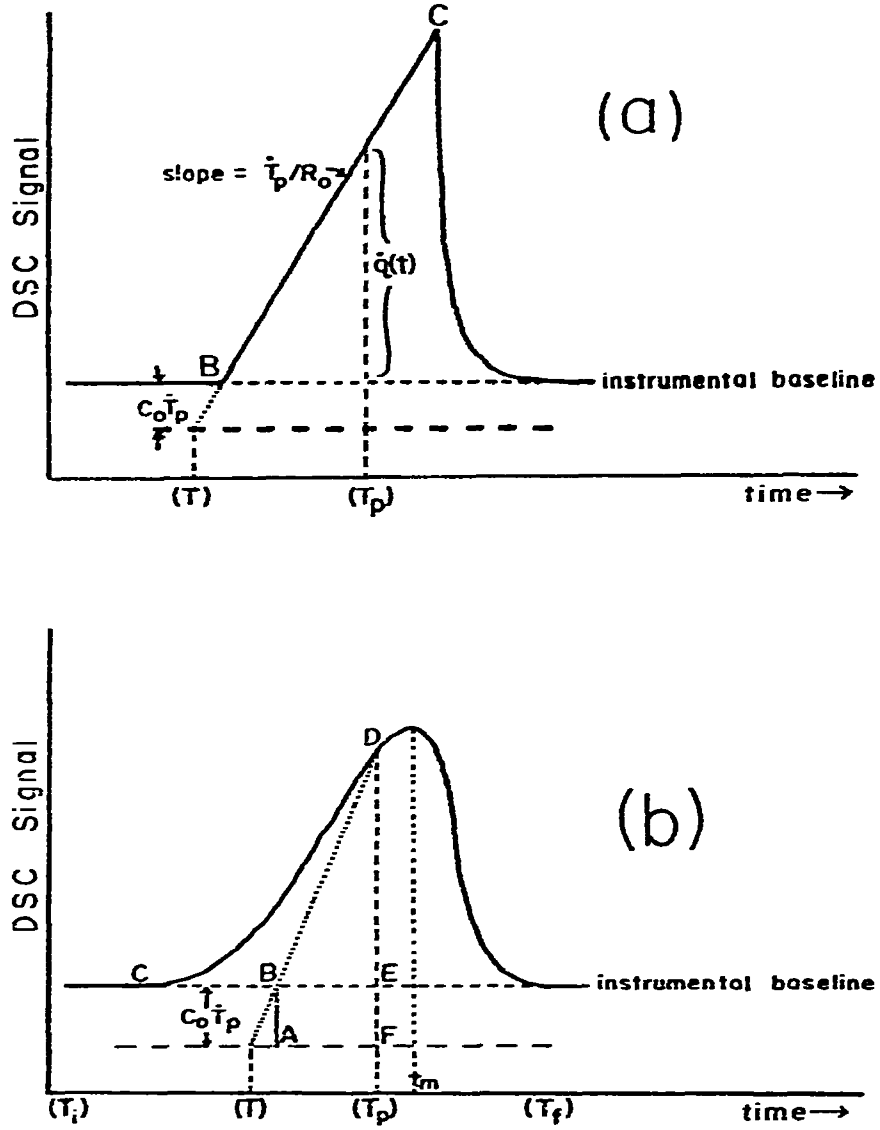

Fig. 1. DSC signal, $\dot{q}(t)$, vs. time while sweeping temperature at a constant rate $\dot{T}_p$ for (a) ideal pure sample, and (b) impure sample. R_0 is the thermal resistance between the sample container and the sample pan, C_0 the specific heat of the sample and its container, and t_m the time at which the sample has completed melting. T_p is the pan temperature, T the sample temperature, and T_i and T_f the initial and final temperatures used in fitting the instrumental baseline.

signal decays with a time constant $\tau_0 = R_0C_0$ as T catches up with T_p. This follows directly from differentiating eqn (8) in this region and substituting from eqn (10) for $\dot{T} - \dot{T}_p$ with $\dot{h} = 0$. Thus, in principle, one could determine R_0 and τ_0 from the rising slope and the decay constant of the melting curve of a pure material.

Figure 1b shows a DSC melting curve for an impure sample. The instrumental baseline is assumed to be straight, but not necessarily horizontal. It is determined by a least-squares fit to a section of the signal immediately following T_i and another section following T_f. The instrumental baseline is subtracted off the data to give the values of $\dot{q}(t)$. $q(t) = \int_0^t \dot{q}(t)\mathrm{d}t$ is also calculated for each point. From eqn (8), the sample temperature is

$$T(t) = T_i + \dot{T}_p t - R_0 \dot{q}(t) - \tau_0 \dot{T}_p \tag{11}$$

The latent heat $L = q(t_f)$, which is the total area in the melting signal above the instrumental baseline[11]. At time t, the fraction molten is the area ABCDFA divided by the latent heat. The fraction molten at time t is

$$\gamma(t) = [q(t) + \tau_0 \dot{q}(t)]/L \tag{12}$$

where $\tau_0 \dot{q}(t)$ is the area ABEF since AB $= C_0 \dot{T}_p$ and $\dot{q}(t)/\mathrm{BE} = \dot{T}_p/R_0$, the slope of line BD.

Equations (11) and (12) give T and $1/\gamma$ from the data provided we know R_0 and τ_0. For the pure sample, these constants are easily determined, but for the impure melting curve, the analysis is not as straightforward. It has been suggested that one determine R_0 from a separate measurement on a pure sample at the same heating rate and sensitivity. However, we found this unsatisfactory for our purposes. Firstly, because one can accurately measure very pure samples only at a very slow rate and not at the rate used for more impure samples, and secondly, it is difficult to exchange samples in the DSC without altering the thermal flow slightly. However, we can determine τ_0 from the data. Let t_m be the time at which $\gamma = 1$. From eqn (12)

$$\tau_0 = [L - q(t_m)]/\dot{q}(t_m) \tag{13}$$

where t_m is obtained from the position of the melting peak. For a given value of R_0, we calculate $T(t)$ and $1/\gamma(t)$ for several points in the melting region. These are fit to eqn (7) by linear least squares techniques giving values for A, B, C, and $\chi^2 \equiv \Sigma_t [T(t) - A - B/\gamma(t) - CT(t)/\gamma(t)]^2$. All points with $1.1 \leq 1/\gamma \leq 50$ are used in the fit. R_0 is then varied until the value of χ^2 is minimized, and thus the "best" A, B, and C are determined from which T_0, k, and χ^2 are calculated. The data and final fit are plotted as in Fig. 3.

We also determine the uncertainty in x_2 due to the scatter of the data from the theoretical expression. In the process of varying R_0, we calculate a range of R_0 over which χ^2 is not significantly altered, σ_{R_0}, and a numerical value for $\mathrm{d}x_2/\mathrm{d}R_0$. Then

$$\sigma_{x_2}^2 = (\mathrm{d}x_2/\mathrm{d}R_0)^2\, \sigma_{R_0}^2 \tag{14}$$

We wish to emphasize, however, that this does not completely include the uncertainty due to the determination of t_m and the uncertainty due to errors in the baseline determination.

The samples were made from 99.9999% pure Pb with small additions of Ag, Au, Pt, or Pd. They were single microtome slices of 20 μm thickness and approximately 2 mg mass. They were contained in standard flat aluminum capsules supplied by

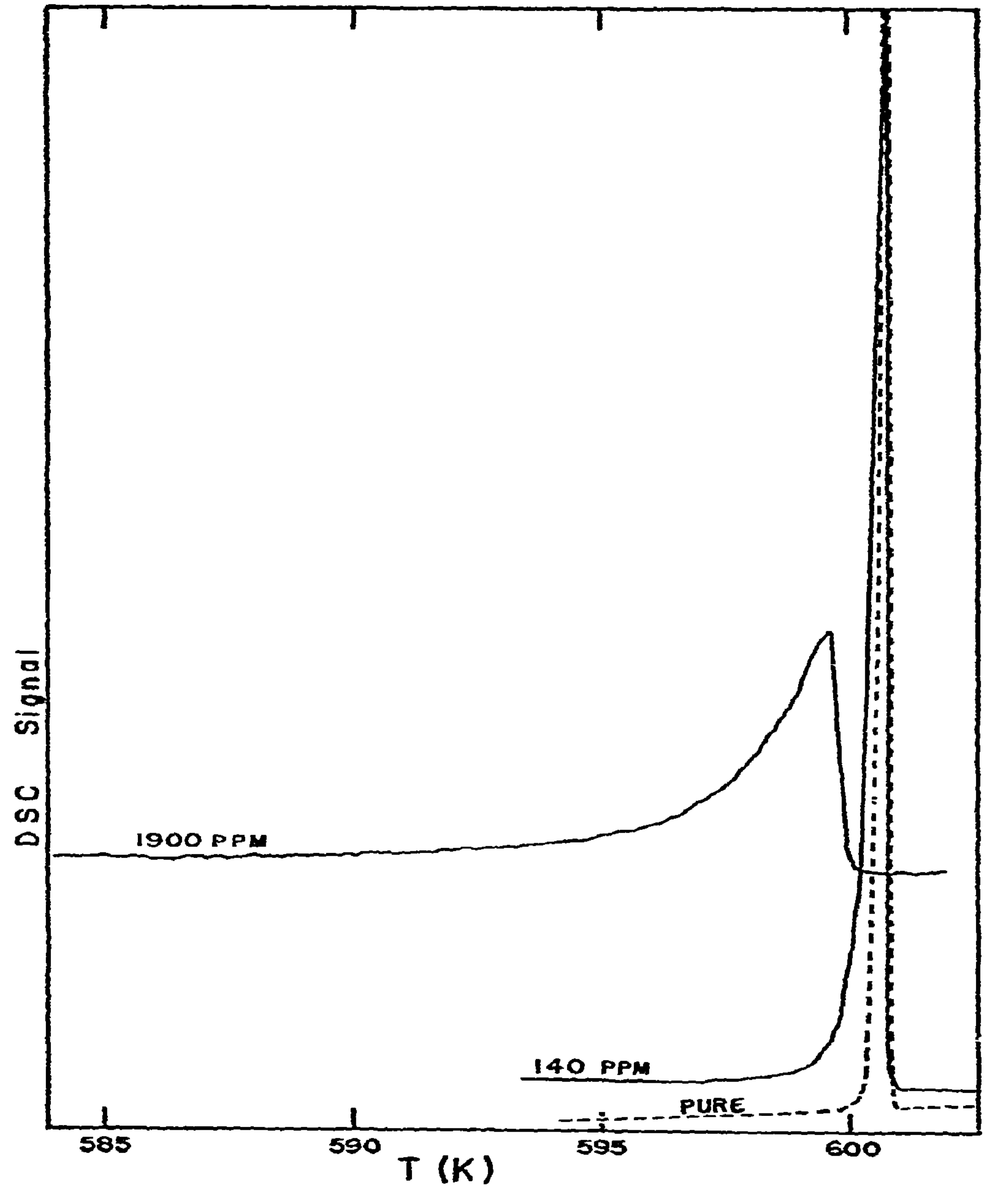

Fig. 2. DSC signal vs. pan temperature for several impurities given in parts per million.

Perkin-Elmer. A slow steady flow of pure N_2 gas through the head was provided on every run, and the heads were cooled with a heat sink kept at a constant temperature of 9.7°C. Temperatures were increased through the melting region at the constant rate $\dot{T}_p$ which was selected in a range from 0.31 deg min^{-1} to 20 deg min^{-1}.

The data were collected and stored by an HP 9810 calculator and analyzed as discussed above with the same calculator. Inputs to the calculator were sample mass, T_i, T_f, $\dot{T}_p$, sensitivity, and a temperature at which the first data point is taken. The calculator was manually started at T_i. The DSC signal was sampled four times per second thereafter and the integrated heat calculated. Periodically, after a selected number of such steps, a point was chosen to use in the fit. A maximum of only 39 such data points could be stored in addition to a point at t_m.

RESULTS

The basic data is the melting curve. In Fig. 2, we display curves of DSC signal

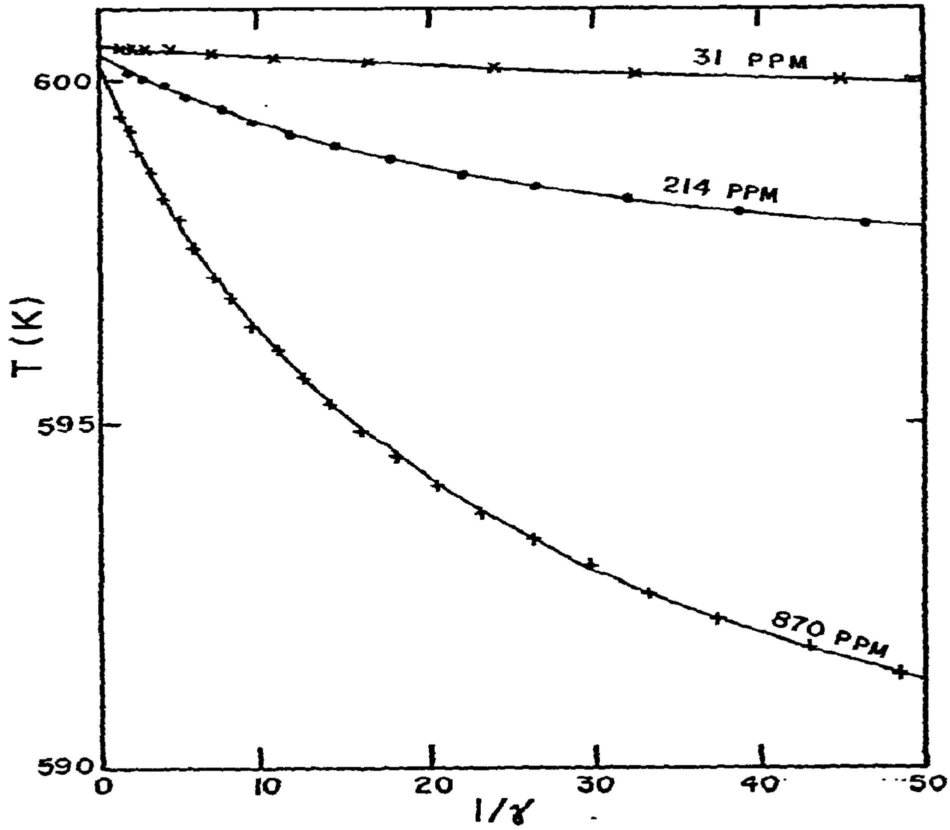

Fig. 3. Sample temperature vs. (fraction molten)$^{-1}$ for three impurities. The curves are the least squares fits to the plotted data points.

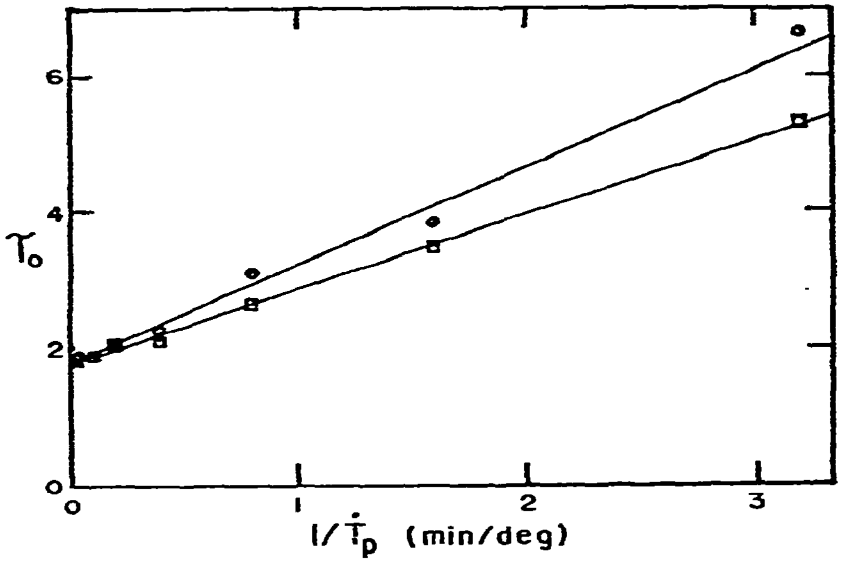

Fig. 4. The time constant τ_0 (sec) vs. $1/\dot{T}_p$ for two different sets of data on Pb(Au)alloy.

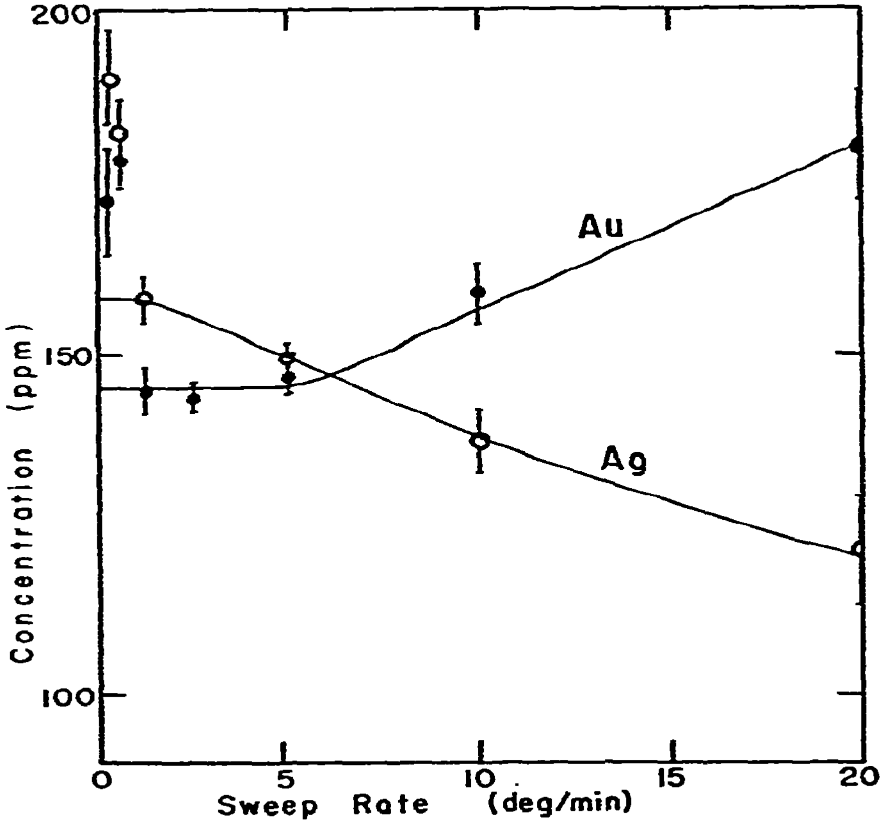

Fig. 5. Rate dependence of the calculated impurity concentration of Ag and Au in Pb.

TABLE 1

COMPARISON OF DSC AND ACTIVATION ANALYSIS MEASUREMENTS OF DILUTE GOLD IMPURITY CONCENTRATIONS IN LEAD

	Calib 1	*Calib 2*	*Calib 3*
x_2 (ppm)			
DSC	147 ± 18	1930 ± 160	19.5 ± 0.6
Act. anal.	143	2970	17.9
k (%)	2.4 ± 1	15 ± 2	1.5 ± 0.3
R_0 (sec K mcal^{-1})	0.42	7 ± 4	0.22
τ_0 (sec)	5.7	5.2	2.8
L (cal g^{-1})	4.21	2.94	5.33

versus pan temperature for three lead samples. The effect of impurities in the lead on the shape of the melting curve is obvious. After analyzing these curves, the data were graphed as sample temperatures versus the reciprocal of the fraction molten as shown in Fig. 3. Again, one can immediately see the effect of impurity concentration on these curves. The lines indicate the best fit of eqn (7) to the data. The intercept at $1/\gamma = 0$ is the melting temperature of pure Pb. The curves cross $1/\gamma = 1$ at the melting temperature of the alloy. The initial slope at $1/\gamma = 0$ gives the solute concentration, and the distribution coefficient is related to the curvature.

The value of R_0, the thermal resistance between the pan and the sample, ranged between 0.20 and 0.25 (sec K mcal^{-1}) for samples containing less than 300 ppm. Above this, the value of R_0 increased with concentration to about 0.5 for 900 ppm impurity concentration and became very large if the concentration exceeded the solid saturation solubility at the eutectic temperature. $\tau_0 = C_0R_0$ varied with the sweep rate as shown in Fig. 4. This is likely due to the flow of N_2 gas which had to be heated and thus contributed to the heat capacity.

Shown in Fig. 5 is the effect of sweep rate on the calculated value of x_2 for both Au and Ag impurities in Pb. It is observed that there is little effect of sweep rate on the calculated Au concentration for $0.5 \leq \dot{T}_p \leq 5$ deg min^{-1}. The Ag measurement does show rate effects for $\dot{T}_p > 1$ deg min^{-1}. The measurements at 0.3 and 0.6 deg min^{-1} are mysterious but may not relate to a physical property of the sample.

Three samples of dilute Pb(Au) alloys were prepared and sent to General Activation Analysis, Inc. for activation analysis of the concentration of Au in each. A microtome slice of each of these was measured by the DSC melting technique. The results are shown in Table 1. A "pure" lead sample gives an impurity concentration of 2 ± 1 ppm which is consistent with its being 99.9999% pure.

DISCUSSION

This method of measuring concentrations of metallic impurities in nearly pure lead is relatively rapid, reproducible, and accurate for concentrations in the range from a few ppm to about 1000 ppm, or the maximum solid solubility, whichever is lowest. The samples need be only 2 mg in size making possible the measurement of spatial variation in the concentration. This technique does not distinguish one impurity from another and may not give an accurate measure of total impurity concentrations if there are many different impurity atoms involved. The minimum measurable concentration is limited by the sensitivity of this method in detecting a change in the shape of the melting curve, but the upper limit is set by breakdown of the theory, if the concentration is above the maximum solubility at the eutectic or by inability to obtain a linear baseline over the large range of temperatures involved in the melting curve. The calibration sample No. 2 contained more Au than is soluble at the eutectic (1160 ppm); thus we could not measure it by this technique. In order to check the reliability of higher concentration measurements, we dissolved 852 ppm Au in a Pb rod and measured the concentration at some 8 points along the rod to get an average concentration of 868 ± 30 ppm in good agreement with the amount introduced.

The values of the distribution coefficient k are all qualitatively correct, for they are very similar to the distribution coefficient at the eutectic. One of the principal uncertainties in this interpretation of the melting signal is the large calculated variation of k with x_2. Thurmond and Struthers[6] show k to vary monotonically with temperature between the eutectic and the melting point. In our case, the value of k as seen in Table 1 seems to approach zero at T_0 and to increase too rapidly as T is lowered, to extrapolate to the correct result at the eutectic.

The effects of sweep rate upon the calculated x_2 probably reflects equilibrium effects. As the alloy melts, the concentration in the remaining solid should decrease, because the solubility of the solute in the liquid is greater than that in the solid. In order to maintain equilibrium, the solute must diffuse out of the solid. The rate that the new equilibrium can be attained is dependent upon the diffusion constant of the solute in the Pb. We have made DSC measurements for dilute Pt, Pd, Au, and Ag alloys of Pb. For Pt, Au, and Pd, the diffusion constant is in the order of 10^6 cm^2 sec^{-1}, and these impurities all give a value of x_2 which is constant for $\dot{T}_p \leq 5$ deg min^{-1}. The diffusion rate of Ag, on the other hand, is an order of magnitude slower, and thus the values of x_2 should be constant for a sweep rate $1/\sqrt{10}$ of the 5 deg min^{-1} found above. We cannot check this prediction directly because of what appears to be instrumental problems at the two lowest sweep rates. As is observed in Fig. 5, there is a sudden increase in x_2 at these two slowest rates. We believe they are instrumental, because the magnitude of the sudden increase depends upon the particular heads used with the DSC, and we can think of no sample-related explanation for this effect. Values of x_2 measured for Pb(Ag) alloys at 1.25 deg min^{-1} do agree very well with the weighed amount of Ag placed in Pb samples and quenched from the melt to avoid segregation problems.

It is concluded that the "linearization" procedure is not the correct way to analyze melting curves for impurity measurements. The procedure here not only gives results that fit the theoretical expression very well, but the results for x_2 do not depend upon the range of $1/\gamma$ used. This range has to be arbitrarily chosen in the "linearization" approach, and x_2 varies by more than an order of magnitude for different regions of $1/\gamma$ between 2 and 50. We chose the entire range $1.1 < 1/\gamma < 50$. We have also taken successful measurements with $1.1 < 1/\gamma < 100$. Therefore, we do not need a set of standards to select a range of $1/\gamma$ as in the "linearization" approach.

If we divide τ_0 in Fig. 4 by R_0, we get the specific heat versus $1/\dot{T}_p$. This specific heat originates from the heat capacity of the lead and its aluminum container and of the N_2 gas that flows through the heads of the DSC. The latter term should appear as $C_g R_g/\dot{T}_p$ where C_g is the specific heat of the gas with a flow rate R_g. This explains the linear dependence of τ_0 on $1/\dot{T}_p$. The intercept at $1/\dot{T}_p = 0$ is $C_0 R_0$. For these samples $R_0 = 0.3$ sec K mcal^{-1}, so we get $C_0 = 5.8$ mcal deg^{-1}. We compare this to 5.6 mcal deg^{-1} for the 26.2 mg of Al and 0.1 mcal deg^{-1} for the 3 mg of Pb and find the agreement very good. We thus conclude that our method of determining τ_0 and R_0 from the melting curve is justified.

ACKNOWLEDGMENT

We wish to thank Dr. J. Bevan Ott of the Brigham Young University Chemistry Department for letting us use his differential scanning calorimeter for this research.

REFERENCES

1 E. E. Marti, *Thermochim. Acta*, 5 (1972) 173.
2 E. M. Barrall, II and R. D. Diller, *Thermochim. Acta*, 1 (1970) 509.
3 G. L. Driscoll, I. N. Duling and F. Magnotta, in R. S. Porter and J. F. Johnson (Eds.), *Analytical Calorimetry*, Plenum, New York., 1968, 271–278.
4 E. F. Palermo and J. Chiu, *Thermochim. Acta*, 14 (1976) 1.
5 S. A. Moros and D. Stewart, *Thermochim. Acta* 14 (1976) 13.
6 Van 't Hoff, *Z. Phys. Chem.*, 1 (1887) 481.
7 G. N. Lewis and M. Randall, *Thermodynamics and the Free Energy of Chemical Substances*, McGraw-Hill, New York, 1923, Ch. 20.
8 C. D. Thurmond and J. D. Struthers, *J. Phys. Chem.*, 57 (1953) 831.
9 S. V. R. Mastrangelo and R. W. Dornte, *J. Am. Chem. Soc.*, 77 (1955) 6200.
10 *Thermal Analysis Newsletter*, No. 5, Perkin-Elmer Corp., Norwalk.
11 H. M. Heuvel and K. C. J. B. Lind, *Anal. Chem.*, 42 (1970) 1044.
12 D. L. Decker, C. T. Candland and H. B. Vanfleet, *Phys. Rev. B*, 11 (1975) 4885.